ISSN 1330-3651
UDC/UDK 620.172.24:[621.874:669.14

# PERFORMANCE ANALYSIS OF SUBSTITUTION OF APPLIED MATERIALS USING FRACTURE MECHANICS PARAMETERS

*Nedeljko Vukojević, Mirsada Oruč, Dušan Vukojević, Fuad Hadžikadunić, Omer Beganović*

Original scientific paper

By replacing the S355 conventional structural steel with V/Nb base micro-alloy steel it is possible to achieve a considerable reduction in the structure mass itself without safety risk, which is also proved by testing fracture mechanics properties of the materials. The numerical results have been also confirmed by analyzing the reliability of the selected materials, with special reference to safety from fracture hazard in the steel welded joints under consideration. Presented in the paper are the results of the numerical evaluation of the bridge crane steel structure under static and dynamic conditions for two steel grades and dimensions. This testing methodology can be applied to any kind of mechanical structure. It can also stress the importance of fracture mechanics application to the evaluation of the condition and behaviour of significant mechanical structures. The immediate effect of this investigation is the saving in the mass of the material used, together with a considerable fracture risk reduction, as well as an improvement in the working properties of the bridge crane steel structure.

***Keywords***: *dynamic response, finite element analysis, fracture mechanics, bridge crane, safety from fracture hazard, welded joint*

## Analiza uspješnosti supstitucije primijenjenog materijala pomoću parametara mehanike loma

Izvorni znanstveni članak

Zamjenom konvencionalnog strukturnog čelika S355 s mikrolegiranim čelikom na bazi V/Nb moguće je postići značajno smanjenje vlastite mase konstrukcije bez ugrožavanja sigurnosti što potvrđuju ispitivanja ponašanja materijala i sa aspekta mehanike loma. Numerička rješenja su potvrđena i kroz analizu sigurnosti izabranih materijala s posebnim osvrtom na aspekt sigurnosti od loma u zavarenom spoju predmetnih čelika. U radu su prikazani rezultati numeričke evaluacije čelične konstrukcije mosne dizalice u statičkim i dinamičkim uvjetima za dva kvaliteta i dvije dimenzije čeličnih limova. Primjenom navedene metodologije ispitivanja, koja se može implementirati na bilo koju vrstu strojarske strukture, kao konačan rezultat istraživanja dobiva se ušteda u masi ugrađenog materijala uz značajno smanjenje opasnosti od pojave loma i uz poboljšanje eksploatacijskih svojstava konstrukcije.

***Ključne riječi:*** *dinamički odziv, mehanika loma, mosna dizalica, numerička analiza, sigurnost od loma, zavareni spoj*

## 1 Introduction
Uvod

Conventional steel plates used for the manufacture of significant mechanical structures have long been in need of replacement in view of increasingly demanding industrial working conditions and needs [1]. The application of low-alloy and micro-alloy steels, as well as special structural shapes, besides a saving in the mass of the material, results in a cheaper transport, lower operating costs, a larger useful load, easier accelerating and braking, potential higher operating speeds, etc.

The introduction of micro-alloy steels brings about a considerable increase in mechanical structure load carrying capacity but also poses a problem concerning the weldability of such steels [2]. Besides high yield stress and strength, micro-alloy steels have good impact toughness even at lower temperatures. A more intensive drop in toughness can be expected in the heat-affected zone (HAZ) due to the grain growth and rapid cooling. Using V/Nb base alloying elements, steels with exceptional tensile and fatigue resistance properties have been obtained, which, using adequate welding technology, can completely replace conventional S355 J2G3 structural steel. This leads to a considerable reduction in the structure mass with an increase in the working performance and safety.

The weld joining the materials under consideration has been experimentally tested. The testing methodology described is aimed at justifying the materials substitution on grounds of an additional increase in safety [3].

The numerical analysis makes it possible to test the main beams of the two-beam bridge crane model for two types of applied materials and two plate widths. This analysis has been carried out in order to test the static load carrying capacity of the structure, and evaluate its dynamic behaviour, the final purpose being to test its structural and geometric parameters [4].

## 2 Experimental part
Eksperimentalni dio

### 2.1 Material properties
Svojstva materijala

For the purpose of carrying out the experimental testing, two types of materials have been used, i.e. S355 J2G3 carbon structural steel, defined in EN 10027-1, having a thickness $\delta$=12 mm and labelled S, and Nb/V-1 micro-alloy steel having a thickness $\delta$=7 mm, labelled ML. The chemical composition of the materials delivered is shown in Tab. 1. The selected specimens labelled S have been welded using MAG ($CO_2$) technique, and those labelled ML, using REL technique.

***Table 1*** *Chemical composition of specimens, mas. %*
***Tabela 1.*** *Kemijski sastav uzoraka u mas. %*

| Specimen | C | Si | Mn | P | S | Cr | V | Nb |
|---|---|---|---|---|---|---|---|---|
| S | 0,21 | 0,53 | 1,47 | 0,038 | 0,029 | - | - | - |
| ML | 0,04 | 0,58 | 0,89 | 0,032 | 0,004 | 0,02 | <0,01 | 0,033 |

The tensile tests have been carried out on the standard rectangular test specimens, defined as ASTM E8-86 [5], with the filler metal in the central section of the work and transversely to the direction of the load application. The Nb/V-1 steel flat specimens tested are labelled Z-ML and the structural steel ones are labelled Z-S. During each testing, three test specimens have been used, the results

being shown in Tab. 2.

***Table 2*** *Mechanical properties of specimens*
***Tabela 2.*** *Mehanička svojstva uzoraka*

| Specimen | Yield stress $R_{p0,2}$ /MPa | Tensile strenght $R_m$/MPa |
|---|---|---|
| Z-ML | 501,5 | 583,6 |
| Z-S | 335,5 | 444,0 |

The analysis of the fractured surfaces shows that ductile fracture has been involved in all these cases. The fracture of the ML test specimens has occurred in the base metals and in close proximity with the heat-affected zone, meaning that the strength of the filler metal is higher than that of the base metals.

The variable load testing technique is defined by the ASTM E466 [6] and E468 [7] standards. The test specimens used for dynamic testing are rectangular in shape. They have been taken from the welded plates, with only the middle of the weld being taken into account.

The dynamic testing is carried out within the force control, the relationship being $\sigma_{min}/\sigma_{max}$=0,1, which corresponds with the character of the variable load application with this type of cranes [8]. The fatigue resistance values achieved for these two test specimens, i.e.

- $S_f$=339,4 MPa - for the ML welded joint and
- $S_f$=279,3 MPa - for the S welded joint,

show that the fatigue resistance of the selected ML welded joint is 21,5 % higher than that of the S selected welded joint (Figs. 1 and 2).

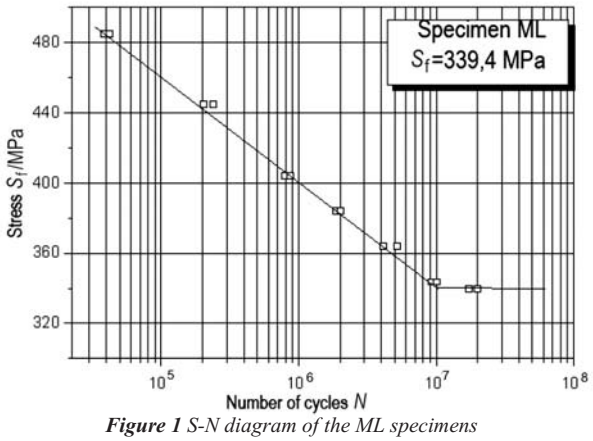


***Figure 1*** *S-N diagram of the ML specimens*
***Slika 1.*** *S-N dijagram od uzorka ML*

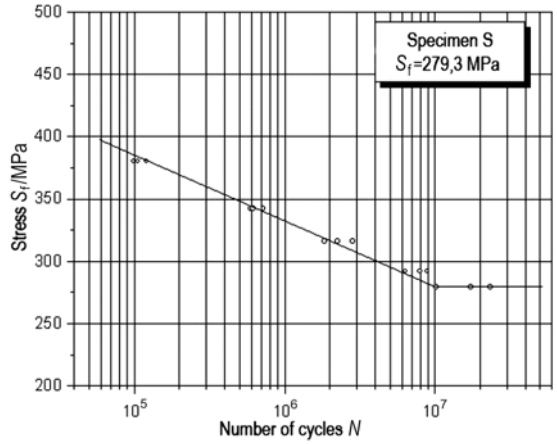


***Figure 2*** *S-N diagram of the S specimens*
***Slika 2.*** *S-N dijagram epruveta od uzorka S*

The impact tests of the ML and S specimens of the welded plates have been carried out with a purpose of determining the overall impact energy ($E$) at +20, –20, –60 °C, as well as that of its components, i.e. the energy absorbed in initiating the fracture ($E_{inic}$), and in its propagation ($E_{prop}$). The procedure of determining the overall impact energy is defined by the ASTM E23 [9] standard.

Figs. 3 and 4 show typical force vs. time curves for the heat-affected zone in the ML and S test specimens.

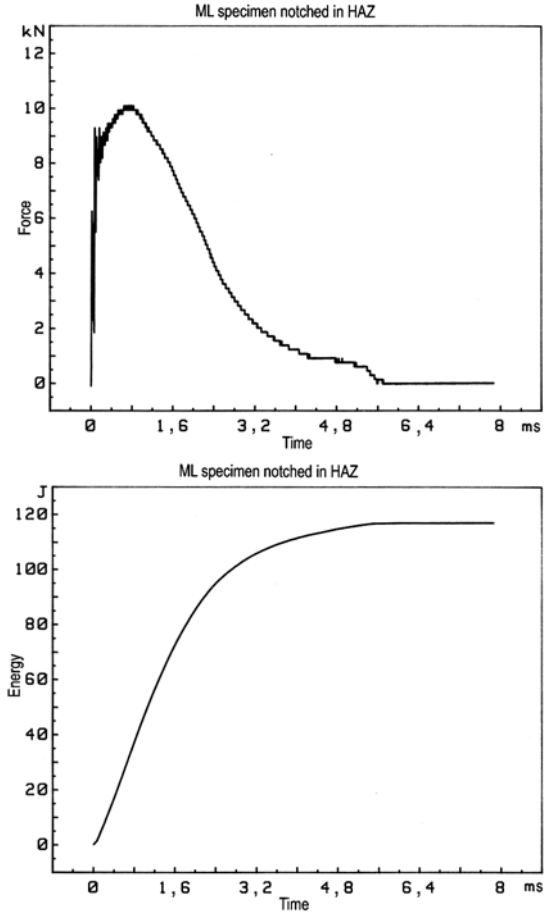


***Figure 3*** *Force vs. time and energy vs. time curves for the ML specimen notched in HAZ*
***Slika 3.*** *Dijagram sila-vrijeme i energija–vrijeme za uzorak ML sa zarezom u ZUT*

The test specimens for the impact tests have been taken along the thickness of the welded joint notched at characteristic parts of the welded joint, i.e. with the notch in the base metal (BM), in the weld metal (WM) and in the heat-affected zone (HAZ). The dimensions of the ML test specimen are 6×8×55 mm, the notch depth being 2 mm, whereas the dimensions of the S test specimen are 8×10×55, its notch depth being also 2 mm. Liquid nitrogen in petrol-ether has been used as a cooling agent. The results of the overall impact energy average values are given in Tab. 3.

A visual inspection of the fractured test specimens shows that the fracture at higher temperatures has been markedly ductile, whereas that at extremely low temperatures has become markedly brittle.

***Table 3*** *Impact energy of the base metal, weld metal and heat affected zone*
***Tabela 3.*** *Energija udara za osnovni metal, metal zavara i ZUT*

| Temp. | Specimen | Base metal | | | Weld metal | | | Heat affected zone | | |
|---|---|---|---|---|---|---|---|---|---|---|
| °C | Energy/J | Total impact energy, $A_u$/J | Crack initiation energy, $A_I$/J | Crack propagation energy, $A_P$/J | Total impact energy, $A_u$/J | Crack initiation energy, $A_I$/J | Crack propagation energy, $A_P$/J | Total impact energy, $A_u$/J | Crack initiation energy, $A_I$/J | Crack propagation energy, $A_P$/J |
| +20 | ML-1 | 130 | 40 | 90 | 95 | 30 | 65 | 112 | 23 | 89 |
| | S-1 | 60 | 24 | 36 | 146 | 63 | 83 | 52 | 20 | 32 |
| –20 | ML-2 | 109 | 35 | 74 | 44 | 25 | 19 | 97 | 23 | 74 |
| | S-2 | 32 | 16 | 16 | 141 | 60 | 81 | 22 | 5 | 17 |
| –60 | ML-3 | 86 | 22 | 64 | 8 | 2 | 6 | 86 | 24 | 61 |
| | S-3 | 4 | 2 | 2 | 7 | 3 | 4 | 15 | 10 | 5 |

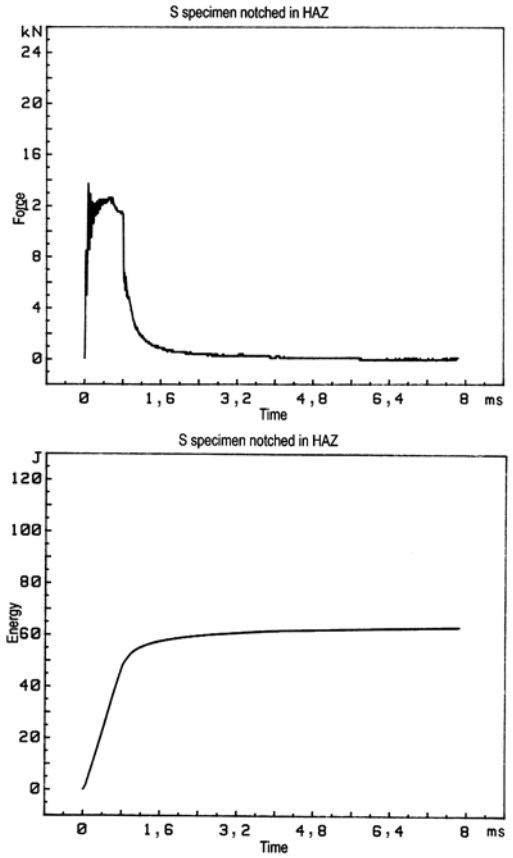


***Figure 4.*** *Force vs. time and energy vs. time curves for the S specimen notched in HAZ*
***Slika 4.*** *Dijagram sila-vrijeme za uzorak S sa zarezom u ZUT*

## 2.2
## Fracture mechanics properties
## Svojstva mehanike loma

Fracture mechanics investigations have made it possible to plot the R-curve and the $J$ - $a$ curve, which consists of the J-integral values for uniform crack extensions $a$.

The experiments have been carried out using a single-specimen procedure, during which the test bar has been subjected to successive partial loading/unloadings, as specified in the ASTM E813 [10] and ASTM E1152 [11] standards. The test has been carried out on three standard CT fracture mechanics test specimens each, with the initial fatigue notches cut at characteristic welded joint sections.

The basic diagrams for the ML and S test specimens notched in the heat-affected zone have been plotted in the $F$ - system of coordinates (force vs. displacement of its point of application) and are shown in Figs. 5 and 6. The J-integral for the expanding crack is calculated by:

$$J_{(i)} = \frac{K_{(i)}^2\left(1-\nu^2\right)}{E} + J_{\mathrm{pl}(i)}, \tag{1}$$

where:
$K_i$ – stress intensity factor, MPa$\sqrt{\mathrm{m}}$
$J_{\mathrm{pl}(i)}$ – J-integral plastic component, kJ/m$^2$
$E$ – modulus of elasticity, MPa
$v$ – Poisson's coefficient.

The characteristic unloading stages on the $J$-$R$ curve serve the purpose of determining the reduction in the test specimen load-carrying capacity. Consequently, it is possible to measure the current crack length by means of the reduction in its load-carrying capacity represented by the relationship between elongation and force extensions on the regression line.

For very slight elongations during a plane state of deformation, the values $K_{\mathrm{Ic}}$ and $J_{\mathrm{Ic}}$ defined at the same point on the $F$-$\delta$ curve are joined by the expression:

$$K_{\mathrm{Ic}} = \sqrt{\frac{J_{\mathrm{Ic}} \cdot E}{1-\nu^2}}. \tag{2}$$

The critical value of the J-integral $J_c$ can be $J_{\mathrm{Ic}}$ defined either in the vicinity of the initial ductile crack propagation or, at the instant when the unstable crack propagation results in separation.

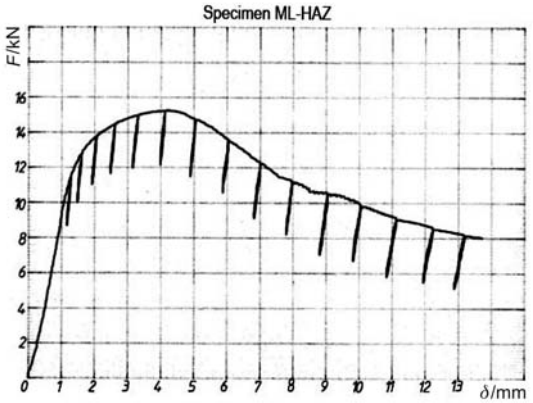


***Figure 5*** *Force-displacement diag. for the ML spec. notched in HAZ*
***Slika 5.*** *Dijagram F-δ epruvete od ML sa zarezom u ZUT*

Figs. 7 and 8 show a characteristic diagram of the $J$-$\Delta a$ curve for the heat-affected zone of the ML and S test specimens plotted by means of the data calculated and the

construction lines in order to determine a deviation from a real stable rupture on the regression line. The critical values of the J-integral $J_{Ic}$ obtained at the intersection of the regression and construction lines are shown in Tab. 4.

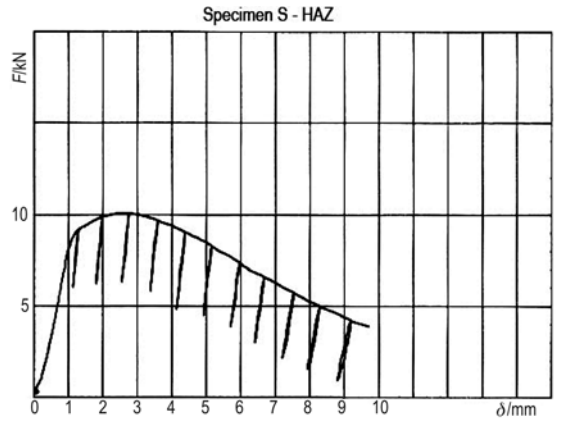


***Figure 6*** *Force-displacement diagram for the S spec. notched in HAZ*
***Slika 6.*** *Dijagram F-δ epruvete od S sa zarezom u ZUT*

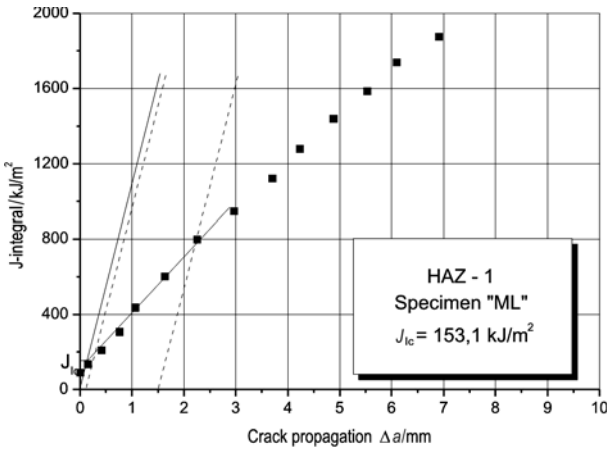


***Figure 7*** *J-Δa diagram for the ML specimen notched in HAZ*
***Slika 7.*** *Dijagram J-Δa epruvete ML sa zarezom u ZUT*

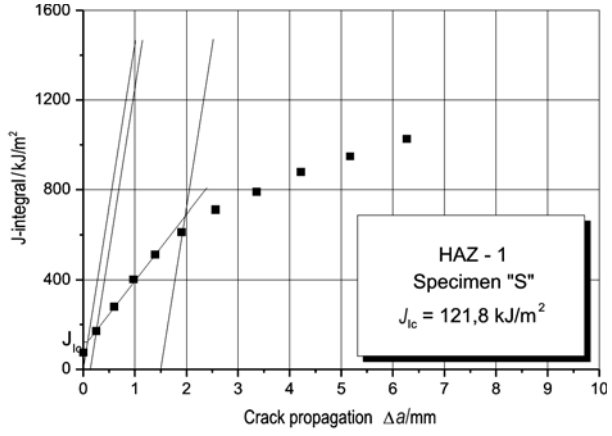


***Figure 8*** *J-Δa diagram for the S specimen notched in HAZ*
***Slika 8.*** *Dijagram J-Δa epruvete S sa zarezom u ZUT*

A critical crack length $a_c$ can be determined using the fracture mechanics equation:

$$K_{Ic} = \sigma \cdot \sqrt{\pi \cdot a_c}, \tag{3}$$

where:
$\sigma = R_{p0,2}$ – yield stress, MPa
$a_c$ – critical crack length, mm
$K_{Ic}$ – critical value of the stress intensity factor during a plane state of deformation, MPa$\sqrt{\text{m}}$.

***Table 4*** *Stress intensity factor and critical crack length*
***Tabela 4.*** *Vrijednosti faktora intenziteta naprezanja i kritične dužine pukotine*

| Specimen | Inicial crack lenght $a$/mm | Critical J-integral $J_{Ic}$/kJ/m$^2$ | Critical stress intensity factor $K_{Ic}$/ MPa$\sqrt{\text{m}}$ | Yield stress $R_{p0,2}$/ MPa | Critical crack lenght $a_c$/mm |
|---|---|---|---|---|---|
| ML-OM | 25,9 | 177 | 202 | 502 | 51,6 |
| ML-ZUT | 27,4 | 153 | 188 | 541 | 38,4 |
| ML-MZ | 26,1 | 157 | 190 | 541 | 39,5 |
| S-OM | 18,6 | 153 | 188 | 336 | 99,9 |
| S-ZUT | 21,0 | 126 | 171 | 373 | 66,6 |
| S-MZ | 21,0 | 143 | 182 | 373 | 75,5 |

The analysis of the fatigue crack propagation calls for introducing fracture mechanics into fatigue investigation. It has been observed that the higher stress causes faster fatigue crack propagation and that the fracture occurs after a smaller number of load alternations. The purpose of determining the fatigue crack propagation rate is to determine the stress intensity scope threshold $\Delta K_{th}$ below which there are no conditions for crack propagation.

To determine the dependence of the fatigue crack propagation rate per cycle d$a$/d$N$ on the stress intensity factor scope $\Delta K$ means to determine the $C$ and $n$ coefficients in Paris equation [13]:

$$\frac{\mathrm{d}a}{\mathrm{d}N} = C \cdot (\Delta K)^n, \tag{4}$$

where:
$\Delta K$ – scope of the stress intensity factor during a plane state of deformation, MPa$\sqrt{\text{m}}$
$C$ - constant,
$n$ - exponent in Paris equation.

The investigation is conducted according to the ASTM E647 standard [12]. This standard recommends measuring the propagation rate of the fatigue crack d$a$/d$N$, developing from the existing crack, and calculating the scope of the stress intensity factor $\Delta K$.

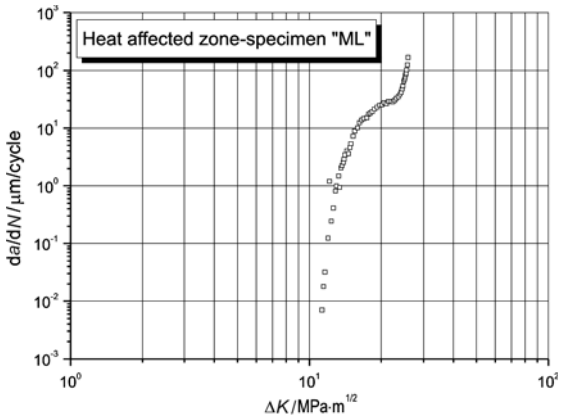


***Figure 9*** d$a$/d$N$ - $\Delta K$ *diagram for the ML specimen notched in HAZ*
***Slika 9.*** *Dijagram ovisnosti* d$a$/d$N$ - $\Delta K$ *epruvete ML sa zarezom u ZUT*

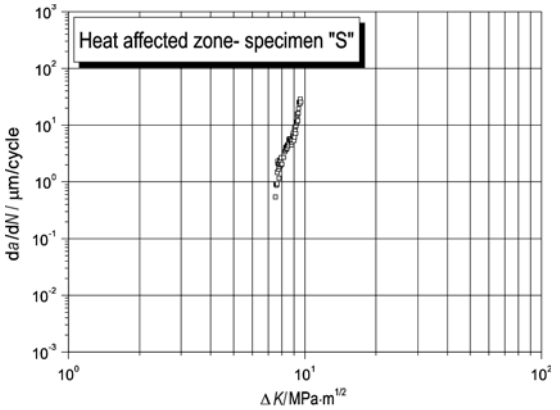


***Figure 10*** d*a*/d*N* - Δ*K diagram for the S specimen notched in HAZ*
***Slika 10.*** *Dijagram ovisnosti* d*a*/d*N* - Δ*K epruvete S sa zarezom u ZUT*

Tab. 5 shows the values of the coefficients *C* (*constant*) and *n* (*exponent*) for the ML and S welded joint test specimens taken from the heat-affected zone. Figs 9 and 10 are typical diagrams showing the dependence of the crack propagation rate on the scope of the stress intensity factor (d*a*/d*N* - Δ*K)* for ML and S specimens notched in the heat-affected zone.

Welded joint toughness should be linked with the change in the inclination of part of the curve in the zone of application of Paris law (middle part of the *S-curve* shown in Figs. 9 and 10). As a rule, materials having a slower crack propagation rate also have a less severe slope on the d*a*/d*N* diagrams.

***Table 5*** *Experimental results of measuring the fatigue crack propagation rate*
***Tabela 5.*** *Rezultati određivanja brzine rasta pukotine*

| Specimen | Treshold $\Delta K_{th}$/MPa $\sqrt{m}$ | Parameter *C* | Parameter *n* |
|---|---|---|---|
| ZUT-ML | 11,2 | $1{,}49 \times 10^{-13}$ | 3,831 |
| ZUT- S | 7,5 | $2{,}53 \times 10^{-11}$ | 3,438 |

## 3
## Finite element analysis
Analiza konačnim elementima
### 3.1
### Numerical model
Numerički model

Using contemporary numerical methods, an ordinary preliminary design of the two-beam bridge crane has been analyzed, and the possibility of replacing the main beam materials has been investigated with the purpose of reducing the overall mass, respecting the prescribed boundary conditions.

In addition to the analysis of the stress-deformation conditions, also applied has been the dynamic analysis of both of the crane model structures, this being an efficient instrument in evaluating the structure behaviour under operating conditions.

A bridge crane having a load-carrying capacity $Q = 70$ kN, and a beam span $L$=19 700 mm (Fig. 11) has been taken as a basic model for a numerical analysis of the behaviour of a real structure.

The main longitudinal beams are made of box-like sections: the preliminary S model is made of the S335 structural steel plate, with a thickness of 12 mm, and the substitution ML model is made of the Nb/V-1 micro-alloy steel plate with a thickness of 7 mm. Tab. 6 shows the basic

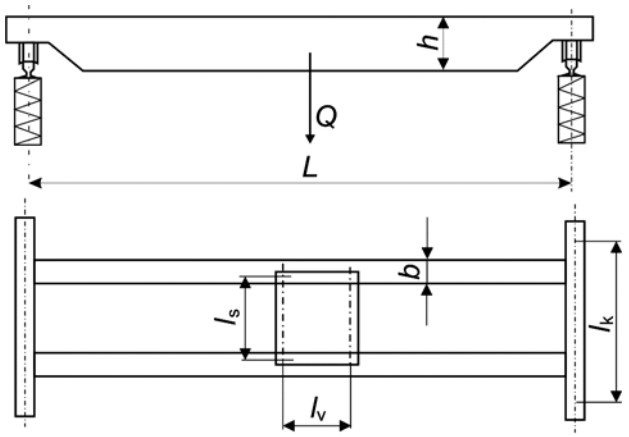


***Figure 11*** *Bridge crane model*
***Slika 11.*** *Model mosne dizalice*

and the modified structure dimensions of these two models.

Fig. 12 shows a finite-element model (FEM) of the preliminary two-beam bridge crane. The FEM analysis has been performed on 12512 2-D finite elements and 12284 nodes. The boundary conditions have been defined in such a way that the main beams have been statically determined and the movement of the wheels prevented. The analysis has been carried out for the effective load position $Q = 70$ kN at the mid-point of the main beam length.

***Table 6*** *Geometrical parameters of the analyzed models*
***Tabela 6.*** *Geometrijski parametri analiziranih modela*

| Index | Rate/mm | Principal dimensions of both models |
|---|---|---|
| $l_k$ | 3000 | wheel span |
| $l_s$ | 1000 | hoist wheel span |
| $l_v$ | 1200 | hoist shaft span |
| $b_S$=$b_{ML}$ | 348 | main beam width |
| Index | Rate/mm | modified dimensions |
| $H_S$ | 762 | model S main beam height |
| $H_{ML}$ | 900 | model ML main beam height |
| $\delta_S$ | 12 | model S vertical plate thickness |
| $\delta_{ML}$ | 7 | model ML vertical plate thickness |

The overall mass of the preliminary model is 8 950 kg, and that of the optimal model 6 198 kg.

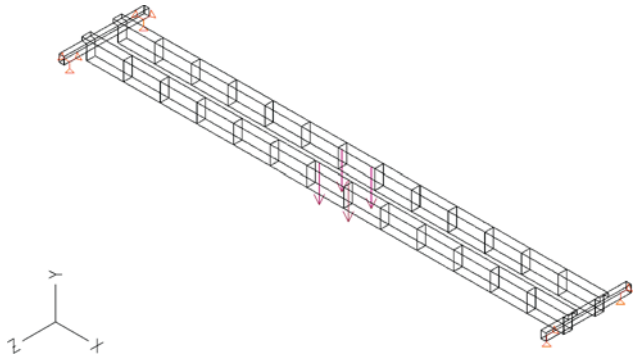

***Figure 12*** *Numerical model of the bridge crane with boundary conditions*
***Slika 12.*** *Numerički model mosne dizalice s graničnim uvjetima*

## 3.2
## Results of FEM analysis
Rezultati analize konačnim elementima

Based on the static and dynamic analyses of the preliminary and modified models of the bridge crane under consideration it is possible to make an overall analysis of the stress-deformation condition values obtained, and of the dynamic behaviour frequency values for the preliminary and modified models.

Fig. 7 shows the stress-deformation condition determined by the numerical analysis. Primarily given are the model deflection values under the nominal load, and the crane weight, after which follow the stress condition values and in particular the values of the equivalent stresses (von Misses), normal stresses and tangential stresses.

The deflection parameters show a reduction, which is satisfactory in terms of the allowable deflection limit of $L/500$. Thus, the bridge crane, after the modification, is within the limits of allowable deflections, safety degree ($S$=1,5), and allowable stresses [14].

The dynamic analysis has been carried out using the method of concentrated masses. It is limited to its own forms since such analysis itself indicates the structure behaviour under compulsory oscillations caused, for instance, by a sudden rise or drop of the weight, etc. The dynamic analysis results are given in Tab. 8, whereas a graphic presentation for the first oscillation mode, appearing on the *x-z* plane is given in Fig. 13.

***Table 7*** *Results of the stress-strain analysis*
***Tabela 7.*** *Rezultati analize naprezanje-deformacije*

| | | |
|---|---|---|
| PRELIMINARY MODEL 348×762 mm, Thickness $\delta$ = 12 mm, specimen S | | |
| The maximum deflection in the middle of the girder: $f$ = 38,3 mm < $f_{allowed}$=39,4 mm | | |
| STRESS, MPa | | |
| Equivalent | Normal, $\sigma$ | Tangential, $\tau$ |
| 77,6 | 77,6 | 45 |
| Allowed stress: $\sigma_{allowed}=R_{eH}/S$=444/1,5=296 MPa | | |
| MODIFIED MODEL 348×900 mm, Thickness $\delta$ = 7 mm, specimen ML | | |
| The maximum deflection in the middle of the girder: $f$ = 33 mm < $f_{allowed}$=39,4 mm | | |
| STRESS/MPa | | |
| Equivalent | Normal, $\sigma$ | Tangential, $\tau$ |
| 105 | 83 | 75,2 |
| Allowed stress: $\sigma_{allowed}=R_{eH}/S$=583/1,5=388 MPa | | |

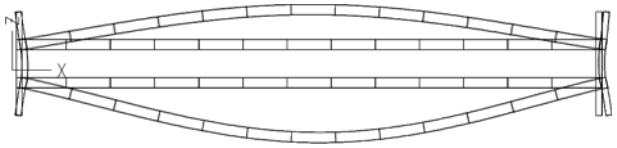

*S model with thickness $\delta$ = 12 mm, the x-z plane, $f_{01}$ = 5,2 Hz*

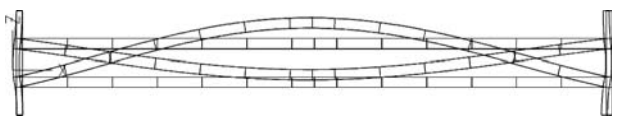

*ML model with thickness $\delta$ = 7 mm, the x-z plane, $f_{01}$ = 6,0 Hz*

***Figure 13*** *Dynamic analysis for the first mode of oscillation*
***Slika 13.*** *Dinamička analiza za prvi mod osciliranja*

The dynamic responses of the structures under consideration within the frequency domain for the impulse on the *y* plane and the response on the *x-y* plane are shown in Figs. 14 and 15, whereas those for the impulse on the *y* plane and the response on the *x-z* plane are shown in Figs. 16 and 17.

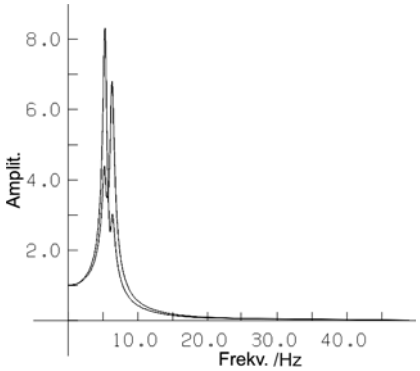


***Figure 14*** *Dynamic response of the preliminary model on the x-y plane*
***Slika 14.*** *Dinamički odziv polaznog modela u x-y ravnini*

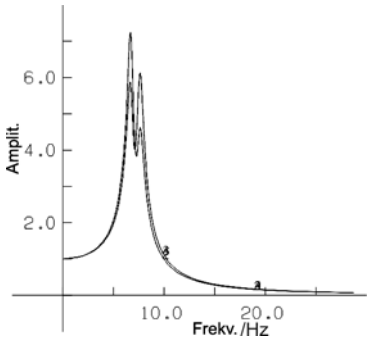


***Figure 15*** *Dynamic response of the modified model on the x-y plane*
***Slika 15.*** *Dinamički odziv modifikovanog modela u x-y ravnini*

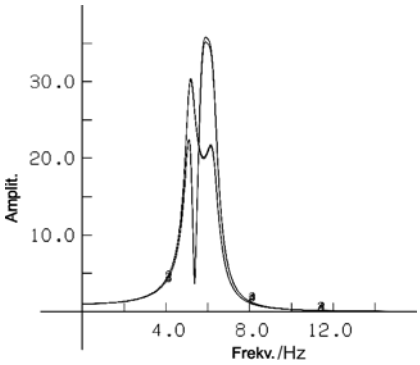


***Figure 16*** *Dynamic response of the preliminary model on the x-z plane*
***Slika 16.*** *Dinamički odziv polaznog modela u x-z ravnini*

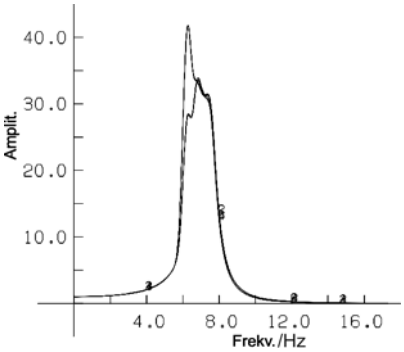


***Figure 17*** *Dynamic response of the modified model on the x-z plane*
***Slika 17.*** *Dinamički odziv modifikovanog modela u x-z ravnini*

According to the results of the dynamic analysis shown in Tab. 8, the models have low values of their

***Table 8*** *Results of the dynamic analysis of the models*
***Tabela 8.*** *Rezultati dinamičke analiza modela*

| PRELIMINARY MODEL 348×762 mm, Thickness $\delta$ = 12 mm | | |
|---|---|---|
| Frequency, Hz | Max. displacement, mm | Impuls plane |
| $f_{01}$ = 5,2 | 0,18 | *x-z* |
| $f_{02}$ = 5,3 | 0,20 | *x-y* |
| $f_{03}$ = 5,7 | 0,19 | *x-z* |
| $f_{04}$ = 6,3 | 0,19 | *x-y* |
| MODIFIED MODEL 348×900 mm, Thickness $\delta$ = 7 mm | | |
| Frequency, Hz | Max. displacement, mm | Impuls plane |
| $f_{01}$ = 6,0 | 0,25 | *x-z* |
| $f_{02}$ = 6,3 | 0,25 | *x-z* |
| $f_{03}$ = 6,7 | 0,21 | *x-y* |
| $f_{04}$ = 7,6 | 0,21 | *x-y* |

own frequencies, which is characteristic of these types of complex structures [4, 8]. With the modified model, a small increase in frequency values has been observed, which has a positive effect.

The frequency analysis shows the dominance of the first frequencies of the model and indicates the structure behavior on the basis of its own oscillation modes. Comparing the structure response on the vertical and horizontal planes for each model taken individually, (Figs. 14 and 16) for the preliminary model and (Figs. 15 and 17) for the modified model, it can be seen that the dynamic coefficient for the response of the structure in the horizontal plane is about five times as large as that for the response of the structure in the vertical plane.

## 3.3
## Analysis of results
Analiza rezultata

The tensile tests have been used as the starting data for the determination of the J-integral. It can be concluded that the ML steel welded joint has considerably higher strength values ($R_{eH}$=501,5 MPa) than the selected S steel welded joint ($R_{eH}$=335,5 MPa). Fatigue resistance values achieved for these two test specimens, show that the fatigue resistance of the selected ML welded joint is 21,5 % higher than that of the S selected welded joint (Figs. 1 and 2).

Decreasing temperature has negative effects on the welded joint impact properties. The values of the overall impact energy of these two materials differ considerably. With almost all samples, except in the heat-affected zone of the S sample at –60 °C, the energy required to initiate a crack is basically lower than that required to expand it. Technically speaking, the higher absorption of energy in crack propagation is more preferable because this prevents the structure from brittle fracture. In other words, the more energy absorbed in crack propagation, the more probability of observing a failure and reacting timely for the purpose of preventing the fracture.

Critical crack length of ML specimens is almost twice the size of critical crack length of the S specimens at all characteristic parts of the welded joint, see Tab. 4.

A slower propagation rate has been noticed on the ML welded joint specimens, because this type of specimen requires a wider scope of the stress intensity factor for the same crack propagation rate. However, on the HAZ-S specimen the crack propagation rate is faster for the same scope of the stress intensity factor.

At higher $K_{Ic}$ values, a faster crack propagation rate is necessary for transition to the brittle fracture zone, as seen in Fig. 9.

Based on the results shown in Tab. 7, it is obvious that an increase in the box-like section height of the main longitudinal beam and a decrease in the wall thickness of the vertical plates have resulted in a stress increase along the complex structure of the bridge crane, but for all that the structure strength requirements have not been neglected.

Comparing the preliminary ($\delta$ = 7 mm) and modified ($\delta$ = 12 mm) models in terms of the frequency analysis, it is noticeable that the modified model has a bit more favorable dynamic factor for the vertical impulse plane (Figs 14 and 15), whereas for the horizontal impulse plane it has worse properties, (Figs 16 and 17).

## 4
## Discussion and conclusions
Razmatranje i zaključak

Based on extensive mechanical investigations, fracture mechanics tests, static and dynamic analyses using the finite element methods for two types of models (preliminary and modified) it can be concluded that an increase in the height of the longitudinal beams cross-section from 792 to 900 mm accompanied by a decrease in the vertical plate thickness from 12 to 7 mm has resulted in a significant reduction in the overall mass of the bridge crane by 30,75 %. The modification has had a beneficial effect on the model deformation properties. The modification has caused a small increase in the structure stress properties but this has been within the limits of allowable stresses. The substitution of the materials and the modification of the longitudinal beams cross section resulted in improved dynamic properties of the structure in terms of its own frequency values. The substitution of the ordinary structural steel with the micro-alloy steel using adequate welding technology has brought about a significant increase in the mechanical properties even at lowered temperatures.

Thus, besides a considerable reduction in the structure mass and the materials cost savings there has been an improvement in the static-dynamic behaviour parameters of the two-beam bridge crane complex structure, in the course of which the introduction of the micro-alloy steel, welded using prescribed technology, has increased the resistance of the structure to brittle fracture and fatigue crack propagation.

**Acknowledgement**
Zahvala
This project was supported by Federal Ministry of Education and Science of Bosnia and Herzegovina under project No. 03-39-5980-50-2/08.

## 5
## References
Literatura

[1] Adamczyk, J. Development of the microalloyed constructional steels. // Journal of Achievements in Materials and Manufacturing Engineering, 14, 1-2 (2006), p.p. 9-20.
[2] Jovičić, R.; Sedmak, A.; Burzić, Z.; Grabulov, V.; Lozanović, J. Structural Integrity Assessment of Ferritic-Austenitic Welded Joints // Faculty of Mechanical Engineering, Belgrade, FME Transactions 36, 1(2008), p.p. 33-37.

[3] Vukojević, N. Istraživanje mogućnosti primjene parametra pukotine u ocjeni integriteta zavarenih čeličnih konstrukcija, Magistarski rad, Mašinski fakultet u Zenici, 2006.
[4] Maneski, T. Kompjutersko modeliranje i proračun struktura. Mašinski fakultet, Beograd, 1998.
[5] ASTM E8-86:1987, Standard Methods of Tension Testing of Metallic Materials. // Annual Book of ASTM Standards, 1987.
[6] ASTM E466:1993, Standard Practice for Conducting Constant Amplitude Axial Fatigue Test of Metallic Materials. // ASTM, 1993.
[7] ASTM E468:1993, Standard Practice for Presentation of Constant Amplitude Fatigue Test Results for Metallic Materials, ASTM, 1993.
[8] Ostrić, D. Dinamika mosnih dizalica. Mašinski fakultet, Beograd, 1998.
[9] ASTM E23: 1986, Standard Method for Notched Bar Impact Testing of Metallic Materials. // Annual Book of ASTM, 1986.
[10] ASTM E813: 1997, Standard Test Method for $J_{Ic}$, A Measure of Fracture Toughness. // ASTM, 1997.
[11] ASTM E1152: Standard Test Method for Determining J-R Curve, ASTM, USA, 1999.,
[12] ASTM E 647: 1995, Standard Test Method for Measurement of Fatigue Crack Growth Rate // ASTM, 1995.
[13] Paris, P.; Erdogan, F. A Critical Analysis of Crack Propagation Laws. // Journal Bas. Eng. Trans. ASME, 1963. p.p. 528.
[14] Šćap, D. Prenosila i dizala-podloge za konstrukciju i proračun. Fakultet strojarstva i brodogradnje, Zagreb, 1988., str. 149-151.
[15] Burzić, Z.; Grabulov, V.; Sedmak, S.; Sedmak, S. Fatigue Properties of a High-Strength-Steel Welded Joint // Materials and technology, 41, 4(2007), p.p. 163–166.

**Authors' addresses**
Adrese autora

***As. Professor dr. sc. Nedeljko Vukojević, mechanical engineer***
University of Zenica
Faculty of Mechanical Engineering
Fakultetska br. 1
72000 Zenica, Bosnia and Herzegovina
Contact:
Phone: +387 32 449 133
Fax: +387 32 246 612
e-mail: vukojevicn@mf.unze.ba

***Professor dr. sc. Mirsada Oruč, metallurgical engineer***
The Metallurgical Institute "Kemal Kapetanović" Zenica
of The University in Zenica
Travnička cesta br. 7
72000 Zenica, Bosnia and Herzegovina

***Professor dr. sc. Dušan Vukojević, mechanical engineer***
University of Zenica
Faculty of Mechanical Engineering
Fakultetska br. 1
72000 Zenica, Bosnia and Herzegovina

***Mr. sc. Fuad Hadžikadunić, mechanical engineer***
University of Zenica
Faculty of Mechanical Engineering
Fakultetska br. 1
72000 Zenica, Bosnia and Herzegovina

***Mr. sc. Omer Beganović, metallurgical engineer***
The Metallurgical Institute "Kemal Kapetanović" Zenica
of The University in Zenica
Travnička cesta br. 7
72000 Zenica, Bosnia and Herzegovina